Modulation of visual gamma oscillation by excitatory drive and the excitation/inhibition balance in the visual cortex.

Orekhova EV[1,2], Sysoeva OV[2], Schneiderman JF[3,4], Lundström S[1], Galuta IA[5], Goiaeva DE[5], Prokofyev AO[2], Riaz B[3,4], Keeler C[3], Hadjikhani N[1,6], Gillberg C[1], Stroganova TA[2,5]

1. University of Gothenburg, Gillberg Neuropsychiatry Centre (GNC), Gothenburg, Sweden;

2. Center for Neurocognitive Research (MEG Center), Moscow State University of Psychology and Education;

3. MedTech West, Gothenburg, Sweden;

4. University of Gothenburg, Inst Neurosci & Physiol, Gothenburg, Sweden;

5. Autism Research Laboratory, Moscow State University of Psychology and Education, Moscow, Russia;

6. Harvard Medical School, MGH/MIT/HST MartinosCenter for Biomedical Imaging, Charlestown, MA USA

Corresponding author:

Elena V Orekhova,

Gillberg Neuropsychiatry Centre

University of Gothenburg

Kungsgatan 12,

SE 411 19 Göteborg, Sweden

Tel. +46 73 591 23 92

Elena.orekhova@gnc.gu.se, orekhova.elena.v@gmail.com

Abstract

Cortical gamma oscillations are generated in circuits that include excitatory (E) and inhibitory (I) neurons. Prominent MEG/EEG gamma oscillations in visual cortex can be induced by static or moving high-contrast edges stimuli. In a previous study in children, we observed that increasing velocity of visual motion substantially accelerated gamma oscillations, and led to the suppression of gamma response magnitude. These velocity-related modulations might reflect the balance between neural excitation induced by increasing excitatory drive, and efficacy of inhibition.

Here, we searched for functional correlates of visual gamma modulations and assessed their development in 75 typically developing individuals aged 7-40 years. Gamma oscillations were measured with MEG in response to high-contrast annular gratings drifting at 1.2, 3.6, or 6.0°/s. In adults, we also recorded pupillary constriction as an indirect measure of excitatory drive.

Pupil constriction increased with increasing velocity, thus suggesting increased excitatory drive to the cortex. Despite drastic developmental changes in gamma frequency and response strength, the magnitude of the velocity-related gamma modulations – a shift to higher frequency and amplitude suppression – remained remarkably stable. Based on the previous simulation studies, we hypothesized that gamma suppression might result from excessively strong excitatory drive caused by increasing motion velocity and reflects a trade-off between overexcited excitatory and inhibitory circuitry. In children, the stronger gamma suppression correlated with higher IQ, suggesting importance of an optimal E/I balance for cognitive functioning.

The velocity-related changes in gamma response may appear useful to assess E/I balance in the visual cortex.

Keywords: MEG, gamma oscillations, excitation/inhibition balance, visual motion, development, IQ

Highlights

- Speeding visual motion increases frequency and suppresses power of gamma.
- Gamma frequency decreases from 7 years on, faster in children than in adults.
- Magnitude of velocity-related modulation remains stable across 7-40 years.
- Gamma suppression correlates with gamma frequency and IQ in children.
- Gamma suppression may reflect efficiency of excitation/inhibition balance.

1. Introduction

Animal studies suggest that a precise balance between excitation and inhibition (E/I balance) in neural networks orchestrates neural activity in space and time, and that this balance is important for cortical functioning (Dorrn, et al., 2010; Isaacson and Scanziani, 2011; Xue, et al., 2014). The fine-tuning of the E/I balance takes place during development (Dorrn, et al., 2010; Froemke, 2015) and is mediated by maturational changes in γ-aminobutyric acid (GABA)- and glutamate-mediated neurotransmission (Carmignoto and Vicini, 1992; Le Magueresse and Monyer, 2013; Piekarski, et al., 2017). Pathological alternations of E/I balance characterize epilepsy (Maheshwari and Noebels, 2014; Mann and Mody, 2008; Wu, et al., 2015) and, according to animal models of neuro-developmental disorders, may represent a key neurophysiological mechanism underlying abnormal perceptual and cognitive processes in neurodevelopmental disorders (LeBlanc and Fagiolini, 2011; Lee, et al., 2017; Nelson and Valakh, 2015; Rubenstein and Merzenich, 2003).

Despite the urgent need for biomarkers of the E/I balance in the human brain (Ecker, et al., 2013; Levin and Nelson, 2015), valid non-invasive measurements are still lacking. Recently, the stimulus-induced high-frequency gamma oscillations in brain activity measured with EEG/MEG have attracted considerable attention as the putative noninvasive indicators of an altered E/I balance in cortical networks (Levin and Nelson, 2015; Nelson and Valakh, 2015). Gamma oscillations (30-100 Hz) are generated by populations of interconnected excitatory and inhibitory neurons in response to sufficiently strong excitatory drive (Buhl, et al., 1998; Munk, et al., 1996). These oscillations critically depend on fast-spiking (FS) parvalbumin-sensitive (PV+) interneurons that are capable of quickly synchronizing activity of the principle cells by inhibiting them through a negative feedback loop (Takada, et al., 2014). Because gamma synchronization depends on the excitatory state of both E and I circuitry, the strength of the gamma response to external input is intimately related to the E/I balance in neural networks. Increasing intensity of the excitatory input usually induces an increasingly strong gamma response, and the gamma oscillations are particularly powerful when excited E circuitry is not properly balanced by inhibition (i.e. in case of high E/I ratio) (see e.g.(Yizhar, et al., 2011).

There has been a number of studies attempting to assess gamma modulation by the intensity of sensory stimulation of different modalities (Rossiter, et al., 2013; Schadow, et al., 2007a; Schadow, et al., 2007b). Visual gamma oscillations recorded by MEG (Hoogenboom, et al., 2006) have been most thoroughly investigated because their strong

heritability (van Pelt, et al., 2012) and highly reliability (Muthukumaraswamy, et al., 2010; Tan, et al., 2016) highlight their potential value as biomarkers. The visual gamma oscillations are thought to be generated through the interaction of principle excitatory cells and fast-spiking inhibitory neurons (so called principal-inhibitory-neuron-gamma or PING) (Vinck, et al., 2013). It has been demonstrated that visually induced MEG gamma activity increases with increasing intensity of the stimulation manipulated by luminance contrast (Hadjipapas, et al., 2015; Hall, et al., 2005; Perry, 2015; Perry, et al., 2015), coherent motion strength (Peiker, et al., 2015; Siegel, et al., 2007), eccentricity (van Pelt and Fries, 2013), or transition from stationary to moving stimulus (Muthukumaraswamy and Singh, 2013; Swettenham, et al., 2009).

In contrast to previously reported results, our recent MEG study in children revealed a strong suppressive effect of increasing stimulus velocity on the gamma response power that was paralleled by a prominent increased in gamma peak frequency (Orekhova, et al., 2015). These unexpected findings imply that highly powerful visual input might cause gamma power suppression instead of enhancement.

Although unexpected, the velocity-related gamma suppression phenomenon resembles that which has been observed in some invasive studies in primates that used visual stimuli of high luminance contrast (Hadjipapas, et al., 2015; Jia, et al., 2013; Roberts, et al., 2013). These studies demonstrate a non-linear bell-shaped dependency of visual gamma power on luminance contrast.

The transition from gamma power enhancement to suppression as a function of input drive can be explained by a computational model of PING gamma oscillations suggested by Borgers and Kopell (Borgers and Kopell, 2005). The transition from low to modest levels of excitatory input to the Inhibitory-cells (I-cells) increases the number of recruited neurons, thereby facilitating gamma oscillations at the populational level, and eliciting an increase in gamma power. However, a too strong excitatory drive may disrupt synchronization between I cells and/or E-I synchronization and lead to a reduction in the power of gamma oscillations. A bell-shaped dependence of gamma power as a function of the strength of excitatory drive is thus expected: an initial increase up to some critical intensity is followed by suppression at yet higher intensities.

In the context of the Borgers and Kopell's model, our findings of gamma suppression suggest that stimuli moving with a sufficiently high speed may result in a failure of the excessively activated I-cells to synchronize network activity, and consequently correspond to a descending branch of the bell-shaped curve. Therefore, the gamma suppression driven by

an increase in stimulus velocity seems to reflect a distinct neural phenomenon, which highlights the nonlinear relationships between external drive, E/I ratio, and gamma power modulation in the human brain. The model predicts that the *stronger and more rapid suppression* of gamma oscillation power at the descending branch of the bell-shaped curve occurs when excitation of the E-cells is effectively reduced by inhibitory synaptic currents, i.e. at a relatively *lower E/I ratio*. On the other hand, weaker and slowly developing gamma suppression is expected in case of higher E/I ratio. Thus, modulation of gamma oscillations by an increase in the stimulus velocity could pave the way to characterization of E/I balance in normal and disturbed visual networks and, if confirmed in systematic studies of typical individuals and individuals with neurodevelopmental conditions may have important clinical implications.

In this study we aimed to characterize the incidence, properties and individual variability of gamma suppression in a large population of neuro-typical children and adults through a broad age range (6 – 40 years), thereby clarifying whether the gamma suppression is age-specific or a more general phenomenon. In order to modulate the excitatory drive to the visual cortex, we used the 'visual motion' paradigm that revealed the paradoxical suppression of gamma power in our previous studies in children (Orekhova, et al., 2015; Stroganova, et al., 2015). We expected that maturation of GABA-, and glutamate-mediated neurotransmission would change the frequency and power of gamma response and affect their modulations as a function of excitatory drive to the cortex.

To confirm that an increase in stimulus velocity elicits higher excitatory input to the visual cortex, we measured pupillary reaction in a subsample of our participants. A transient constriction of the pupil can be provoked by visual motion without increment in light flux, reflecting an increase in the neuronal activity within the visual cortical areas (Barbur, et al., 1998; Sahraie and Barbur, 1997; Wilhelm, et al., 2002). Therefore, if faster motion of the annular grating does intensify excitatory drive to the visual cortex, it is likely to be accompanied by greater constriction of the pupil.

An important prediction derived from Borgers and Kopell's model (Borgers and Kopell, 2005; Cannon, et al., 2014) is a link between a magnitude of gamma suppression and the efficacy of neural inhibition in the visual cortex. Here, we addressed this prediction in two ways. First, because relatively high excitability of inhibitory neurons should facilitate gamma suppression and accelerate gamma oscillations (Ferando and Mody, 2015; Mann and Mody, 2010), we expected that the magnitude of gamma suppression would correlate with individual variations in gamma frequency. Second, because more efficient inhibition in the

visual cortex was shown to be related to better visual perceptual skills and higher IQ (Cook, et al., 2016; Melnick, et al., 2013), we expected that magnitude of suppression of gamma oscillations in response to increasing velocity of visual motion will correlate positively with IQ.

2. Material and methods

2.1. Participants

2.1.1.Children

Fifty typically developing boys between 6 to 15 years of age were recruited for the study from local schools in Moscow. The inclusion criterion was absence of neurological or psychiatric diagnoses. In all but one child (his parents refused the additional visit for IQ assessment) the IQ was assessed with the Kaufman Assessment Battery for Children KABC II (Kaufman and Kaufman, 2004).

Two control children were later excluded from the MEG data analysis. One of the two had excessive myogenic artifacts during MEG recording and another one failed to follow the instruction to respond with a button press. Of the 48 boys left, two were later excluded from the group analysis due to the reasons described in the Results section. This resulted in a final sample size of 46 children (age range 6.7 – 15.5 years, mean 11.0 years, SD = 2.2).

The investigation was approved by the Ethical Committee of the Moscow University of Psychology and Education. All children provided their verbal assent to participate in the study and were informed about their right to withdraw from the study at any time during the testing. Written informed consent was also obtained from a parent/guardian of each child.

2.1.2. Adults

The initial adult sample included twenty seven adult subjects. Twenty two adult participants were recruited in Gothenburg. The inclusion criterion was an absence of reported neurological or psychiatric conditions. One male subject (20 years-old) was later excluded from the MEG group analysis because of a post-hoc discovery of an unreported epilepsy. His results are described separately. The age of the other 26 adult participants (3 females) ranged from 19.2 to 40.1 years (mean 27.9 years, SD=6.3). In 20 of 26 the participants (all males) the IQ has been assessed using Wechsler Adult Intelligence Scale, 4th Edition (WAIS-IV)(Wechsler, 2010).

The study was approved by the Gothenburg Regional Ethical Review Board (Regionala etikprövningsnämnden i Göteborg). All participants gave written informed consent after the experimental procedures had been fully explained.

2.2. Experimental task

We applied the same experimental paradigm as that used in our previous studies in children (Orekhova, et al., 2015; Stroganova, et al., 2015). The subjects sat in a dim magnetically shielded room, with their head resting against the back of and positioned as closely as possible to the top of, the helmet-shaped surface of the helium dewar. For children, we used a PT-D7700E-K DLP projector that presented images with 1280 x 1024 screen resolution and 60 Hz refresh rate. For adults, the stimuli were presented using FL35 LED DPL projector with 1920 x 1080 screen resolution and 120 Hz refresh rate. The stimuli consisted of black and white annular gratings with a spatial frequency of 1.66 circles per degree of visual angle and outer diameter of 18 degrees of visual angle (Fig. 1A, insert). They were generated using Presentation software (Neurobehavioral Systems Inc., USA). The grating appeared in the center of the screen over black background and drifted to the central point at one of the three velocities: 1.2°/s; 3.6°/s; 6.0°/s, referred to below as 'slow', 'medium' and 'fast'. The frequencies of black to white transitions at a given position in the visual field produced by these velocities were 4, 12, and 20 Hz, respectively.

Each trial began with the presentation of a white fixation cross in the centrum of the display over a black background for 1200 ms, that was followed by a moving grating. After moving for a random interval varying between 1200 and 3000 ms, the stimulus stopped and remained on the screen for the length of the 'response period'. The response period was individually adjusted in children (see (Orekhova, et al., 2015) for details) and was fixed at 1000 ms in adults. To keep participants alert, we instructed them to detect termination of the motion and to respond by pressing a button as soon as the motion stopped. If no response occurred within the response period the grating was substituted by a discouraging message "too late!" (in Russian/Swedish for participants in Moscow/Gothenburg) that remained on the screen for 2000 ms, after which a new trial begun. The participants were instructed to constantly maintain their gaze at the fixation cross in the intervals between the stimuli.

Individual omission and commission (responses that occurred during motion or earlier than 150 ms following termination of motion) errors were measured in all

participants except two children for whom the behavioral responses were not recorded due to equipment error. The error trials were excluded from the MEG analysis.

The experiment included three blocks of trials; stimuli of different velocities were presented in all three blocks in a random order. The participants responded with either the right or left hand (50% trials each) in a sequence that was counterbalanced between blocks and participants. Each stimulus velocity was presented 30 times within each experimental block resulting in 90 trials per stimulus velocity. In order to minimize visual and mental fatigue, short (3-6 s) animated cartoon characters were presented between every 2-5 stimuli. The subjects' head position was continuously monitored and adjusted to a common position using MaxFilter™ (v2.2).

2.3. Pupillometry

Pupil size was measured in 19 of 27 adult participants using an EyeLink 1000 binocular tracker. We calculated the amplitude of the maximal pupil constriction (i.e., minimal pupil size) during the 0 to 1200 ms stimulus interval as a percentage of the average pupil size during the- 100 to 0 ms pre-stimulus interval:

$$\% \text{ relative constriction} = (A_{pre\text{-}mean} - A_{post\text{-}min})/A_{pre\text{-}mean} * 100$$

These values were averaged separately for slow, medium and fast conditions. Trials contaminated by blinks in the window of interest (-100 to 1200 ms), those preceded by cartoons and error trials were excluded from analysis.

2.4. MEG recording

In children, neuro-magnetic brain activity was recorded at the Moscow MEG Centre (the Moscow State University of Psychology and Education) using a 306-channel detector array (Vectorview; Neuromag, Helsinki, Finland) positioned in a magnetically shielded room (AK3b; Vacuumschmelze, Hanau, Germany). In adults, MEG was recorded at the NatMEG Centre (The Swedish National Facility for Magnetoencephalography, KarolinskaInstitutet, Stockholm) using a similar 306-channel system (ElektaNeuromag TRIUX) located in 2-layer magnetically shielded room (Vacuumschmelze GmbH). Both systems comprise 102 identical triple sensor elements. Each sensor element consists of three superconducting quantum interference devices, two with orthogonal planar gradiometer pickup coils and one with a magnetometer pickup coil configuration. Four electrooculogram (EOG) electrodes were used

to record horizontal and vertical eye movements. EOG electrodes were placed at the outer canti of the eyes and above and below the left eye. To monitor the heartbeats in children one ECG electrode was placed at the manubrium sterni and the other at the mid-axillary line (V6 ECG lead). In adults the ECG electrodes were placed at left and right sides of the chest under the collarbone. MEG, EOG, and ECG signals were recorded with a band-pass filter of 0.03–330 Hz in Moscow and 0.1-330 Hz in Stockholm, digitized at 1000 Hz, and stored for off-line analysis.

2.5. MEG data preprocessing

The data was first de-noised using the Temporal Signal-Space Separation (tSSS) method (Taulu and Hari, 2009) implemented in MaxFilter™ (v2.2) with parameters: '-st'=4 and '-corr'=0.90. For all three experimental blocks, the head origin position was adjusted to the initial head origin position in the block #2. For further pre-processing we used the MNE-python toolbox (Gramfort, et al., 2013) and custom Python and Matlab scripts.

The de-noised data was filtered between 1 and 145 Hz. To remove biological artifacts (blinks, heart beats, and in some cases myogenic activity), we then applied independent component analysis (ICA). The MEG periods with too high (4000e-13 *fT/cm* for gradiometers and 4e-12 *fT* for magnetometers in adults, 4000e-13 *fT/cm* for gradiometers and 8e-12 *fT* for magnetometers in children) or too flat (0.1e-12 *fT/cm* for gradiometers and 1e-13 *fT* for magnetometers) amplitudes were excluded from the analysis. The number of independent components was set at dimensionality of the raw 'SSS'ed' data (usually around 70). We further used an automated MNE-python procedure to detect artificial EOG and ECG components, which we complemented with visual inspection of the ICA results. The number of rejected artifact components was normally 1 for vertical eye movements, 0-3 for cardiac and 0-6 for myogenic artifacts.

The artifact-corrected data was epoched from -1.0 to 1.2 s relative to the stimulus onset. The epochs containing strong muscle artifacts were excluded by thresholding the mean absolute value of the high-frequency (>70 Hz) signal. The threshold was set at 3 standard deviations from the power of the 70-Hz high-passed signal averaged across channels. The epochs left were visually inspected for the presence of undetected high-amplitude bursts of myogenic activity and the epochs contaminated by such artifacts were manually marked and excluded from the analysis. The number of artifact-free epochs with correct button-press responses for the 'slow', 'medium' and 'fast' conditions was on average 70.5, 70.8 and 70.5 in children and 79.7, 79.3 and 78 in adults.

2.6. Time-frequency analysis at the sensor level

The time-frequency analysis at the sensor level has been performed in all participants. In this study only planar gradiometers were analyzed. For spectral estimation we used multitaper analysis with discrete prolate spheroidal sequences (DPSS). We estimated the spectra in overlapping windows of 400 ms (shifted by 50 ms) at frequencies from 2.5 to 120 Hz. The frequency step was 2.5 Hz, the number of cycles was set at frequency/2.5 and the bandwidth was 4, which resulted in spectral smoothing ±5 Hz around each center frequency. To decrease the contribution of phase-locked activity related to the appearance of the stimulus on the screen, as well as photic driving that could be induced by the temporal frequency of the stimulation and screen refresh rate (or their interaction), we subtracted averaged evoked responses from each single data epoch using 'subtract_evoked' MNE function.

The relative gamma response (in dB) was estimated in 400-1000 ms post-stimulus period relative to the -700 to -200 ms period of pre-stimulus baseline (central points of the 400 ms spectral window) using the 'tfr_multitaper' MNE-python function. The individual gamma response frequency and power were assessed at the gradiometer sensor pair with the maximal average response. To identify the location of the 'maximal response sensor pair' the power changes were averaged over the two gradiometers of each sensors triplet, over the 400-1000 ms post-stimulus period and over frequencies of the gamma range (50-110 Hz in children and 35-100 Hz in adults). Because our previous study showed that detectable gamma response on the group level is observed at posterior gradiometer sensors (with the maximum at the 'MEG2112/3' pair of gradiometers), the location of the maximal increase in gamma power was defined at one of the selected posterior locations ('MEG1932/3', 'MEG1922/3', 'MEG2042/3', 'MEG2032/3', 'MEG2112/3', 'MEG2122/3', 'MEG2342/3' and 'MEG2332/3'), separately for each condition.

To assess individual gamma peak frequency we first defined the frequency bin with the maximal power of the gamma response. Because the spectra of the gamma responses were not always perfectly Gaussian, we adjusted the peak frequency by calculating a weighted average over whose frequency bins (subject/condition-specific band) where the post-stimulus/baseline ratio exceeded 2/3 of the absolute maximum. The weighted gamma peak power was calculated in dB, as 10*log10(post-stimulus/baseline), where post-stimulus/baseline is an average ratio over these frequency bins.

To assess the reliability of stimulus-related increase in gamma power in each subject and for each velocity condition we compared the single epochs' average pre- and post-stimulus power at the frequency bin of the maximal gamma response using Mann–Whitney U test.

2.7. Time-frequency analysis at the source level

The structural MRIs (1 mm^3 T1-weighted) were available for 23 of 28 adult participants. For these participants we performed source analysis using FieldTrip open source software (http://www.ru.nl/neuroimaging/fieldtrip/). We sought to check for the similarity between gamma response parameters measured at the source and the sensor levels, as well as to assess position of the most significant gamma increase ('maximally induced voxel') in each of the velocity conditions. Prior to analysis each subject's brain has been morphed to the MNI template brain using linear normalization and 0.6 mm grid. To perform source localization we then adapted the two-step approach. As the first step time-frequency analysis was performed on the artifact-free epochs (-0.9 to -0.1 pre-stimulus and 0.4 to 1.2 post-stimulus) using multitaper method. The analysis window was centered at the sensor-defined subject/condition specific frequency ±25 Hz. The DICS inverse-solution algorithm (Gross, et al., 2001) was used to derive the common source spatial filters. Subsequently, bootstrap resampling source statistics was performed (with 10000 Monte Carlo repetitions) to verify for each participant and condition presence of a significant ($p<0.05$) brain cluster of poststimulus increase of gamma power in the visual cortex (L/R cuneus, lingual, occipital superior, middle occipital, inferior occipital, or calcarine areas according to the AAL atlas (Tzourio-Mazoyer, et al., 2002)).

At the second step the signal was filtered in 30-120 Hz range, the 'virtual sensors' time series were extracted for each participant and velocity condition from each of 6855 brain voxels, and the time-frequency analysis (multitaper method, ±5 Hz smoothing, ~1Hz frequency resolution) has been performed. The voxel with the most significant post-stimulus increase of 45-90 Hz power in visual cortex was found. The gamma response parameters were defined for the average of this and the 25 closest voxels. To assess the source-derived gamma response frequency and amplitude we calculated post-/pre-stimulus ratio for each frequency in the broad gamma range (30-120 Hz) and then assessed weighted subject/condition specific frequency and amplitude using the approach applied in the sensor space.

2.8. Statistical analysis

Statistical analysis was performed using STATISTICA-13 software (Dell Inc, 2015). To test for the effect of the velocity condition (hereafter Velocity) on MEG parameters and pupil contraction amplitude, we used the repeated measures analysis of variance (ANOVA). The Greenhouse-Geisser correction for violation of sphericity has been applied when appropriate. The original degrees of freedom and corrected p-values are reported together with epsilon (ε). Partial eta-squared (η^2) was calculated to estimate effect sizes. ANOVA was also used to assess the effect of age group. Spearman coefficients were used to calculate correlations between variables. Details about the statistical analysis are given in the Results section.

3. Results

3.1. Pupil constriction

The repeated measures ANOVA revealed a highly reliable effect of the Velocity ($F_{(2, 36)}$=16.9, $\varepsilon = 0.92$, p<0.0001; η^2=0.48). The magnitude of pupil constriction increased with increasing motion velocity of the annular grating (Fig. 1).

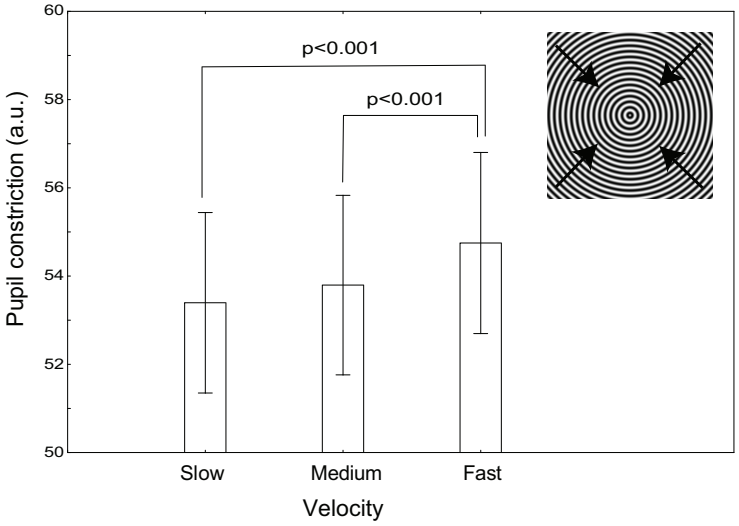

Figure 1. Pupillary constriction response to the annular gratings drifting towards the center of the display at three different velocities ('Slow' - 1.2 °/s, 'Medium' - 3.6 °/s; and 'Fast' - 6.0 °/s). Vertical bars denote 0.95 confidence intervals. The insert shows the stimulus display; the arrows indicate motion direction.

3.2. Incidence of gamma responses to visual motion in the sensor space in children and adults.

Group average time-frequency plots in children and adults are shown in figure 2. These plots are based on 46 children and 26 adults, (2 children and 1 adult participant were excluded from the group analysis due to the reasons described below).

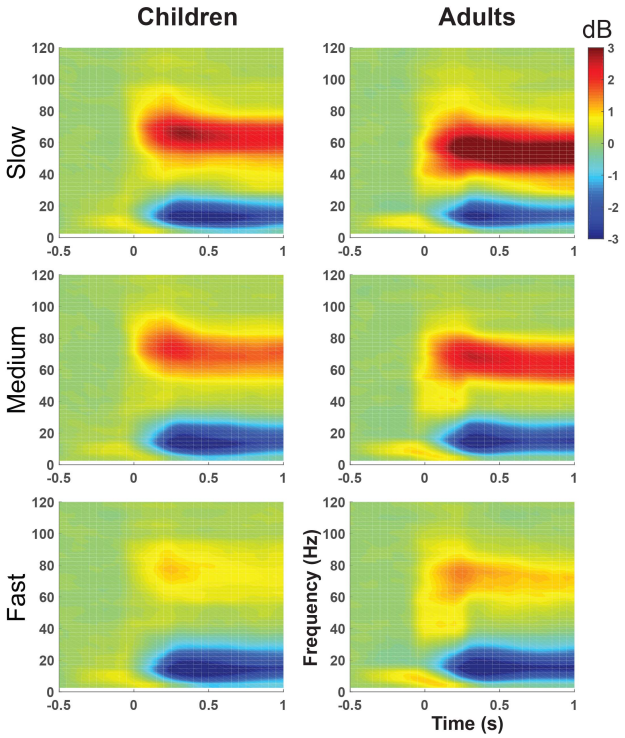

Figure 2. Grand average time-frequency plots for the three velocity conditions in children and adults.

Table 1 shows the number of subjects who demonstrated stimulation-related increases in the gamma power at p<0.05 and p<0.0001 probability levels.

Table 1. Incidence, mean frequency and mean power of motion-related gamma responses detected at different p-levels (Mann-Whitney U test) in children and adults.

	P<0.05			P<0.0001		
	Children, N=46					
Stimulus velocity	Frequency (Hz)	Power (dB)	N and % sample	Frequency (Hz)	Power (dB)	N and % sample
Slow	66.1(6.1)*	3.1(2.0)	45, 98%	65.2 (5.3)	3.6 (1.8)	37, 80%
Medium	73.2(8.5)	2.2(1.8)	43, 94%	72.3 (8.0)	2.8 (1.8)	31, 67%
Fast	82.2(10.8)	1.3(1.0)	37, 80%	79.6 (7.4)	1.9 (1.1)	21, 46%
	Adults, N=26					
Stimulus velocity	Frequency (Hz)	Power (dB)	N and % sample	Frequency (Hz)	Power (dB)	N and % sample
Slow	55.7(5.7)	3.8(1.4)	26, 100%	55.7(5.7)	3.8(1.4)	26, 100%
Medium	65.1(6.0)	2.6(1.3)	26, 100%	65.1(6.0)	2.6(1.3)	26, 100%
Fast	70.0 (8.5)	1.3 (0.7)	26, 100%	69.5 (5.4)	1.5 (0.7)	19, 73%

* Standard deviations are given in parentheses.

Under the slow and medium velocity conditions, gamma response peaks were highly reliable (response vs. baseline: p<0.0001) in all the adults and in the majority of the children. For the third velocity, the highly reliable peaks were detected in the majority of the adults and in about half of the children.

3.3. Comparison of the source- and sensor-derived gamma power and amplitude.

The source analysis was performed in 23 of 26 adults for whom the structural MRI data were available. The DICS beamformer analysis showed presence of a significant cluster of gamma increase in visual cortex in response to the 'slow' and 'medium' Velocity in all these participants. In response to the 'fast' Velocity, a significant cluster was present in 19 of 23 participants. In all three conditions, the most frequent location of the 'maximally induced voxel' was in the calcarine sulcus (in 17/23 subjects in the 'slow' condition, in 16/23 subjects in the 'medium' condition and in 11/18 subjects in the 'fast' condition, see also the *Supplementary table 1* for the MNI coordinates of gamma response for each subject). Figure 3 illustrates source distribution of the gamma response obtained using DICS beamforming technique. No significant shift of the 'maximally induced voxel' in either x, y or z coordinate has been observed between the three velocity condition (rmANOVA: all p's>0.4). The mean intra-individual distance between 'maximally induced voxels' was 5.4 mm (sd=6.2) for the 'slow' vs 'medium' conditions, 10 mm (sd=7.6) for the 'medium' vs 'fast' conditions, and 9.3 mm (sd=8.5) for the 'slow' vs 'fast' conditions. The group average [x y z] position of the 'maximally induced voxel' in the MNI coordinates was [0.0 -93.7 -0.7] for the 'slow' condition, [-0.6 -94.0 -0.7] for the medium condition and [2 -94.7 0.0] for the fast condition. Considering 6 mm spatial resolution of the grid the mean position of the gamma response maximum corresponded to the same MNI template voxel in the left calcarine gyrus in all three conditions.

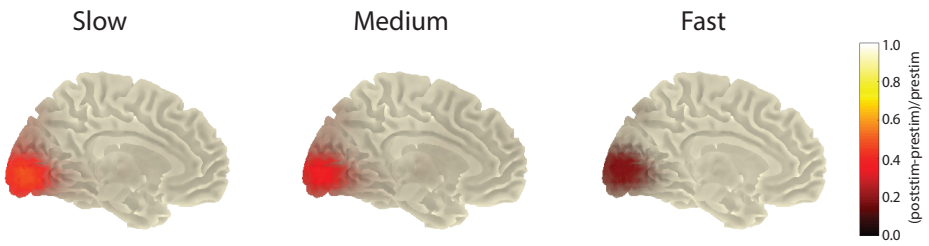

Figure 3. Source localization of the gamma response in the three velocity conditions in adults: the grand average.

Table 2. Spearman correlations between source- and sensor-derived gamma response frequency (F) and power (P) parameters measured in 'slow', 'medium' and 'fast' velocity conditions.

	Source F_{slow}	Source F_{medium}	Source F_{fast}	Source P_{slow}	Source P_{medium}	Source P_{fast}
Sensor F_{slow}	0.96 (N=23*)					
Sensor F_{medium}		0.93(N=23)				
Sensor F_{fast}			0.83 (N=18)			
Sensor P_{slow}				0.79 (N=23)		
Sensor P_{medium}					0.91 (N=23)	
Sensor P_{fast}						0.91 (N=23)

* Only subjects with reliable gamma increase at both sensor and source levels were included into the frequency correlation analysis.

The high correlations between source- and sensor-derived gamma response parameters (Tab. 2) suggest close correspondence between sensor- and source-derived results. Moreover, source-space analysis showed that in all velocity conditions the major source of gamma oscillations was situated in the overlapping regions of the primary visual cortex. Considering that the structural MRI data were not available for all of the participants we further restricted analysis to the sensor space data.

3.4. Velocity-related modulations of gamma oscillations, their variability and outliers

3.4.1. Power

Here and in all further statistical analyses that examined the effect of velocity on the gamma response power at the group level, we included only those participants who demonstrated the reliable ($p<0.0001$) gamma peaks under the 'slow' condition. This strict criterion was applied because the magnitude of the velocity-related power suppression can be reliably estimated only when a reliable gamma response under the slow velocity condition is present. This criterion did not affect the size of the adult sample, but reduced the number of children in the analysis (adults: 26, children: 37). The children excluded from the gamma power modulation analysis (n=9; mean age=9.4 years; range: 6.7 to 12.6 years) were significantly younger (M-W test: $z=2.33$; $p=0.02$) than the rest of the children in the sample (n=37; mean age=11.4; range: 7.7 to 15.5 years).

The majority of participants, regardless of age, demonstrated gradual attenuation of gamma response with increasing stimulus velocity from 'slow' to 'medium' and further to 'fast' (Fig. 4A). Two examples of typical gamma spectra are shown in Figure 5A. In a few subjects, the transition from 'slow' to 'medium' condition elicited an increase (or no change)

in gamma power, succeeded by its decrease under the 'fast' condition (Fig. 5B). One adult and two children showed virtually no change in gamma response power, even at the highest velocity (Fig. 5C, see also Fig.4A, dashed lines). Visual inspection of the MEG record of the adult subject (20 years old) with the atypical lack of gamma suppression has shown presence of the spike-and-wave complexes over the posterior brain regions. Post-hoc examination revealed that he had an unreported diagnosis of epilepsy. The post-hoc inspection of the MRI of one of the two children lacking the gamma suppression (13 years-old; his spectra are pictured in Fig. 5C, upper panel) by a clinical neuro-radiologist revealed presence of Arnold-Chiari malformation. The other child who did not suppress the gamma response with increasing motion velocity (7 years old) has not had a formal medical diagnosis; however, he suffered from minor motor ticks and frequent nightmares according to the parental report.

The two children and one adult who had post-hoc revealed medical conditions and displayed atypical lack of gamma suppression were excluded from all the further group analyses.

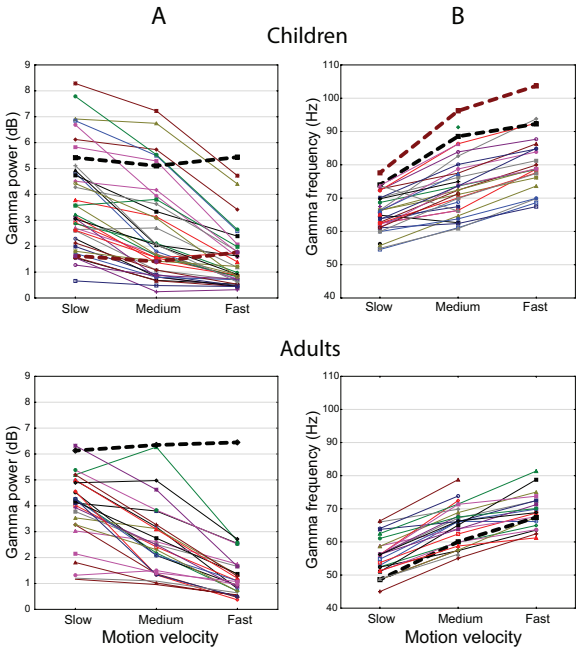

Figure 4. Velocity-related changes in gamma response power and frequency: individual subjects plots. **A.** Gamma response power. Only children with reliable ($p<0.0001$) gamma response under the 'slow' velocity condition are included. **B.** Gamma frequency. The data are shown only for reliable gamma peaks. The thick dashed lines correspond to subjects lacking the power suppression.

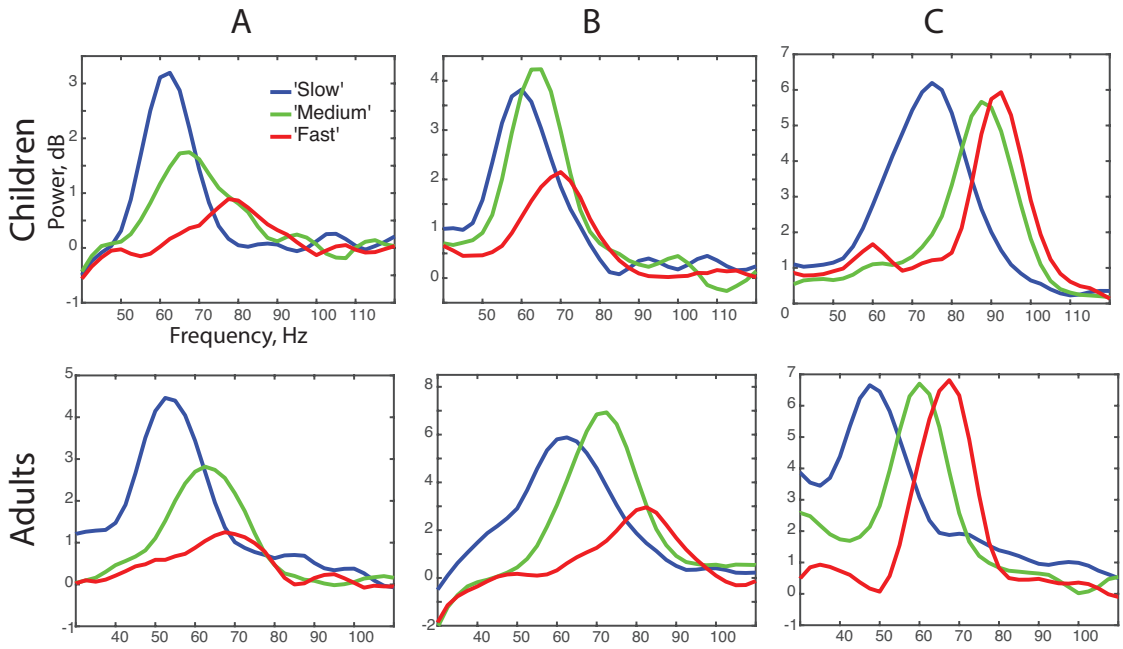

Figure 5. Individual spectra of visual gamma responses and their modulation by motion velocity in children and adults: typical (**A**) and infrequent/atypical (**B** and **C**) gamma response modulations.

In children the repeated measures ANOVA revealed a profound reduction of gamma response power with transition from the 'slow' to the 'medium' and further to the 'fast' condition ($F_{(2,72)}$=93.0, ε=0.8, $p<10e^{-6}$; η^2=0.73; Fig. 6A).

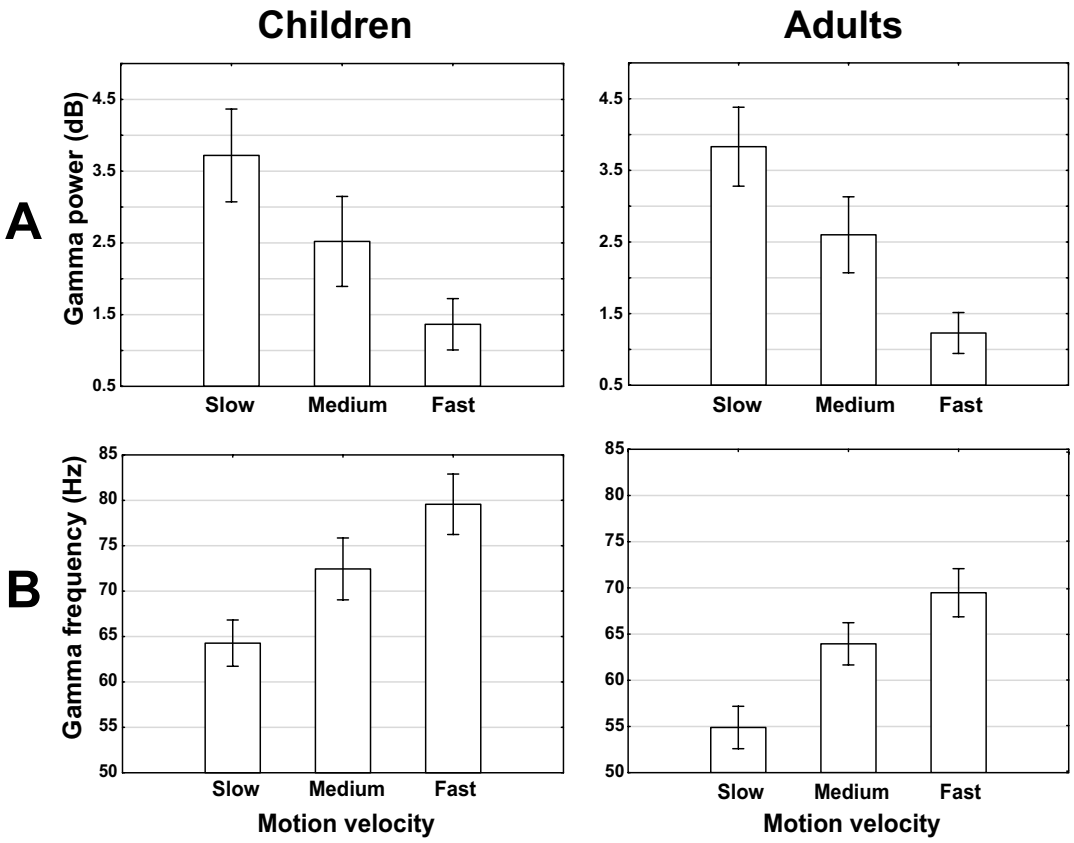

Figure 6. Changes in gamma response power (**A**) and frequency (**B**) as a function of motion velocity in children and adults. Vertical bars denote 95% confidence intervals.

In adults the repeated measures ANOVA also showed highly reliable reduction of gamma response power with changing velocity from 'slow' to 'medium' and further to 'fast' condition ($F_{(2,50)}$=83.1, ε=0.83, $p<10e^{-6}$; η^2=0.77; Fig. 6A).

3.3.2. Frequency

A viable estimate of the gamma peak frequency is possible only when the peak is reliable. We estimated the frequency of an individual gamma response peak only if the stimulus-induced power enhancement was significant at the p<0.0001 level. For the analysis of the velocity effect on gamma frequency ('frequency ANOVA'), we included those participants who had the reliable peaks under all three experimental conditions (21 children, 19 adults).

In children we observed a robust effect of visual motion velocity on gamma frequency ($F_{(2,40)}$=173.6, ε=0.8, $p<10e^{-6}$;η^2=0.9). The gamma peak frequency increased from the 'slow' through the 'medium' to the 'fast' condition (Fig. 6B); the difference between the 'slow' and the 'fast' conditions was 15.3 Hz on average. The robust increase in gamma frequency was also observed in adults ($F_{(2,36)}$=145.9, ε=0.8, $p<10e^{-6}$; η^2=0.89) where it was 14.6 Hz on average.

3.4. Effect of age on gamma oscillations.

3.4.1. Power

The magnitude of the stimulus-induced gamma response significantly increased with age in children between 6 and 15 years, but did not change in adults between 19 and 40 years (Tab. 3). In figure 7A we present the age-related changes in power of gamma response for the 'slow' condition.

Table 3. Spearman correlations between magnitude of the stimulus-induced gamma response (in dB) and age in children and adults.

Stimulus velocity	Children (N=46)	Adults (N=26)
Slow	**0.43****	-0.07
Medium	**0.43****	-0.13
Fast	**0.37***	-0.30

* p<0.05, **p<0.01

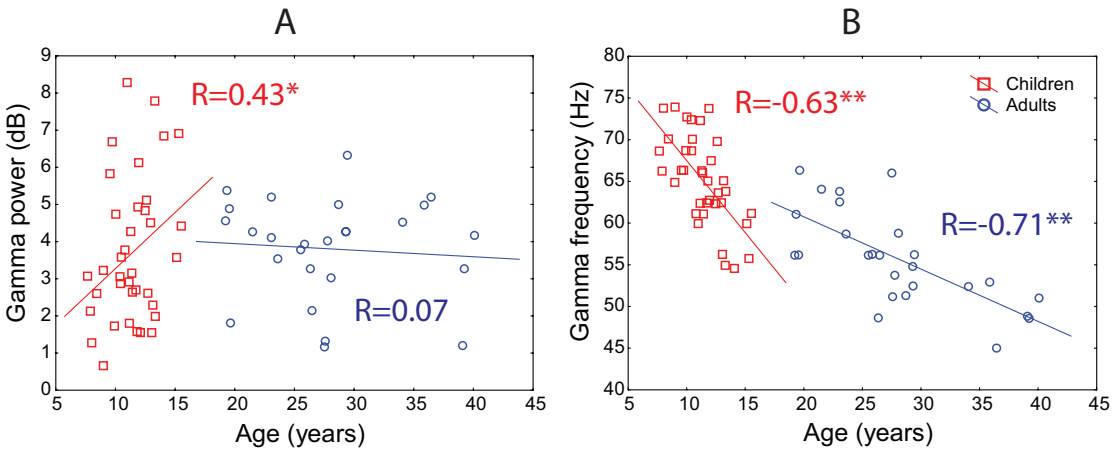

Figure 7. Developmental changes of gamma response power (**A**) and frequency (**B**) in children and adults: slow velocity condition. Asterisks denote the significance of Spearman correlations: *p<0.01; ** p<0.0001

To analyze possible differences in velocity-related changes of gamma response magnitude in children and adults, we performed an ANOVA with the main factor Age-Group (adults, children) and repeated measures factor Velocity (3 conditions). This revealed a highly significant effect of Velocity ($F_{(2, 122)}$=172.8, ε=0.87, p<1e^{-6}; η^2=0.74), but no effect for the Age-Group or the Age-Group*Velocity interaction (p's>0.6).

3.4.2. Frequency

In both the child and the adult samples, the gamma peak frequency decreased with age (Tab 3). In figure 7B we present the age dependent changes in the peak frequency of gamma response induced by 'slowly' drifting gratings. Notably, the drop in gamma frequency was more rapid during childhood (1.712 Hz per year) than during adulthood (0.644 Hz per year). The homogeneity of slopes analysis revealed significant difference between gamma frequency age-related slopes in children and adults for the 'slow' ($F_{(1, 59)}$=7.8, p<0.005, η^2=0.13) and the 'fast' ($F_{(1, 36)}$=7.5, p<0.01, η^2=0.17) velocity conditions, but did not reach significance level for the 'medium' condition ($F_{(1,53)}$=1.3, p>0.1, η^2=0.03). Inspection of figure 7B suggests that the decrease of gamma frequency in adults takes place mainly after 25 years of age, and might reflect aging-related processes.

Table 4. Spearman correlations between gamma response frequency and age in children and adults.

Stimulus velocity	Children	Adults
Slow	**-0.63*** ** (N=37)	**-0.71*** ** (N=26)
Medium	**-0.39*** (N=31)	**-0.74*** ** (N=26)
Fast	**-0.54*** (N=21)	-0.42 (N=19)

* p<0.05, ***p<0.0001

To analyze possible differences in velocity-related changes of gamma frequency in children and adults we performed an ANOVA with factors Age-Group (adults, children) and Velocity (3 conditions). The ANOVA revealed highly significant effects of both Age-Group ($F_{(1, 38)}$=27.1, p<0.0001; η^2=0.42) and Velocity ($F_{(2, 76)}$=317.2,ε=0.81, p<1e^{-6}; η^2=0.89), but no Age-Group*Velocity interaction (p=0.4), suggesting developmental stability of velocity-related increase in gamma frequency.

3.5. Gamma power suppression and gamma frequency

Based on the animal data and computational model reviewed in the introduction, we anticipated that subjects with relatively higher gamma frequency and/or greater velocity-related increase of gamma frequency (i.e. those who might have greater excitation of I neurons or greater velocity-related increase in their excitation) would demonstrate 1) greater overall magnitude of gamma power suppression with transition from 'slow' to 'fast' velocity and/or 2) more 'rapid' gamma power suppression that would occur already at a milder level of excitatory drive (with transition from 'slow' to 'medium' velocity).

To assess gamma power suppression, we introduced two parameters. The first one - gamma Suppression Magnitude (gSM) characterizes degree of gamma power response

suppression with transition from 'slow' to 'fast' condition, normalized by the 'slow' gamma power:

$$gSM = (POW_{slow} - POW_{fast}) / POW_{slow}.$$

The normalization eliminates inter-individual differences in magnitude of gamma oscillations that might be explained by age, anatomical factors, etc. Note, that the positive gSM values characterize gamma suppression.

The second measure - gamma Suppression Slope (gSS) - was calculated as

$$gSS = (POW_{slow} - POW_{medium}) / (POW_{slow} - POW_{fast}).$$

and characterizes how fast with increasing velocity the gamma suppression occurs. Considering that the denominator was positive in all the participants included in the analysis, the gSS was positive if the suppression took place already at the 'medium' velocity. It was negative in the case of initial power increase in the 'medium' velocity condition with the following decrease in the 'fast' condition (e.g. Fig. 5B).

The POWslow, POWmedium and POWfast were calculates as an absolute difference between mean post-stimulus and baseline power in the respective condition and for the subject/condition-specific band (see Methods). The higher gSM value indicates stronger gamma suppression with increasing excitatory drive. The higher gSS value signifies that the relatively greater part of the gamma suppression occurs already with the moderate excitatory drive (i.e. at the 'medium' velocity).

When all subjects with the reliable gamma response in the 'slow' condition ($p<0.0001$) were included into analysis, in children gSS correlated positively with gamma frequency in the 'fast' ($R=0.6$, $p<0.01$) and 'medium' ($R-0.36$, $p=0.05$) conditions (Tab. 5.) These correlations could not be accounted for by age, because gSS did not significantly change with age ($R(29)=-0.3$, $p>0.1$). This means that children who had higher frequency of gamma oscillations at high and medium velocity, suppressed gamma response more rapidly, i.e. already at the transition from the 'slow' to the 'medium' velocity. Unlike that in children, no correlations with gamma response frequency were found in adults (Tab.5) .

We further tested whether the velocity-related changes in gamma response amplitude correlated with changes in gamma frequency. In adults, the slow-to-medium

change in frequency correlated positively with both gSS (R= 0.44, N=26, p<0.05) and gSM (R=0.43,N=26, p<0.05), while the slow-to-fast frequency growth tended to correlate with gSM (R=0.43, N=19, p=0.07)

Table 5. Spearman correlations between gamma suppression parameters (gSM, gSS) and gamma response frequency measured in the three velocity conditions.

	Children				
	F_{slow}, N=37#	F_{medium}, N=30	F_{fast}, N=21	F_{medium} - F_{slow}, N=30	F_{fast}- F_{slow}, N=21
gSM	0.11	0.05	-0.09	0.12	-0.17
gSS	0.25	0.36	**0.60****	0.19	0.26
	Adults				
	F_{slow}, N=26	F_{medium}, N=26	F_{fast}, N=19	F_{medium} - F_{slow}, N=26	F_{fast}- F_{slow}, N=19
gSM	-0.34	-0.07	-0.29	**0.44***	0.43
gSS	-0.25	0.04	-0.14	**0.43***	0.22

*p<0.05, **p<0.01.

Note that the number of subjects included in each analysis depends on the presence of a reliable gamma peak in the corresponding velocity condition.

3.6. Gamma power suppression and IQ

In children, the KABC-II Mental Processing Composite (MPC) IQ score correlated positively with both gSM and gSS (N=36; gSM: R=0.33, p<0.05, gSS: R=0.54, p<0.001; Tab.6). The gSS also correlated positively with KABC-II Simultaneous IQ Score (R=0.51, p<0.01). These correlations suggest that children with higher IQ show greater and more rapid suppression of gamma response with increasing excitatory drive.

Pattern of correlations between MPC IQ and gamma response magnitude in separate velocity conditions suggests that the correlation with gSM and gSS are mainly driven by gamma response power in the 'medium' and 'fast' conditions ('slow': R(36)=-0.07, n.s., 'medium': R(36) = -0.31 (p=0.06), 'fast': R(36)=-0.29, p=0.09).

Table 6. Spearman correlations between gamma suppression parameters (gSM, gSS) and IQ scores.

	Children, KABC II, N=36			Adults, WAIS IV N=17
	Sequential/ Short-Term Memory'	Simultaneous/ Visual Processing	Mental Processing Composite	Total IQ
gSM	0.13	0.28	**0.33***	0.1
gSS	0.15	**0.51****	**0.54*****	0.2

*p<0.05, **p<0.01, ***p<0.001

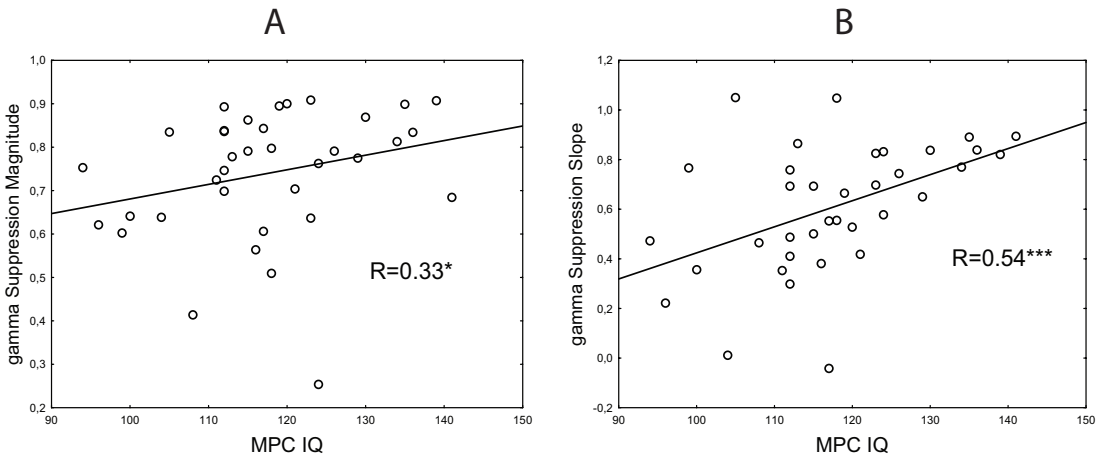

Figure 8. The relationship between gamma suppression parameters and IQ in children. Asterisks denote the significance of Spearman correlations: *p<0.01; ** p<0.0001

No correlations between gamma suppression parameters and IQ reached significance level in adults.

4. Discussion

The current study examined the paradoxical suppression of visual gamma oscillations caused by increasing velocity of drifting annular gratings. In a large sample of children, we replicated our previous findings (Orekhova, et al., 2015) indicating a negative correlation of the visual motion velocity with the magnitude of gamma power enhancement and its positive correlation with the frequency of gamma oscillations We also found the same effects in adults. The pupillometry findings suggest that the effect of velocity on gamma oscillations may be at least partly mediated by changes in excitatory drive. We further investigated developmental stability of this phenomenon and its functional correlates. Despite profound

developmental transformation in absolute values of gamma response frequency and power, the magnitude of velocity-related gamma power and frequency modulations remained stable from middle childhood to adulthood. Based on previous modeling studies, we hypothesized that the suppression of gamma power with increasingly strong excitatory drive reflects the capacity of inhibitory neurons to counteract excitation in the visual networks (i.e., the E/I ratio). Since the E/I ratio depends, amongst other factors, on the tonic excitability of inhibitory neurons, which in turn strongly affects the frequency of gamma oscillations, we expected that the suppression of gamma power would correlate with gamma frequency parameters. Following the prediction from the model of (Borgers and Kopell, 2005), we anticipated that the greater suppression of gamma power would reflect lower E/I ratio that might be beneficial for an individual subject's level of cognitive functioning (Cook, et al., 2016; Melnick, et al., 2013). These predictions were confirmed in children, but only partially in adults, suggesting that E/I balance may be based on different mechanisms during childhood and adulthood.

4.1. Gamma parameters in the source and sensor space.

Comparison of the source and sensor analysis results shows close correspondence of the gamma parameters measured in the source and sensor space. This result agrees well with the findings of Tan et al (Tan, et al., 2016) who reported high reliability of both source- and sensor-derived parameters of visual gamma response and their close correspondence.

Importantly, in all three velocity conditions, the individual maxima of gamma responses were most frequently located in the primary visual cortex (calcarine gyri, see Supplementary Materials) and we did not find any evidence for a systematic shift of the maximum with changes in motion velocity. These findings suggest that generation of gamma activity in all three velocity conditions was based on activity of the same neural circuits.

4.2. Developmental changes in strength and frequency of visual gamma response

Visual stimulation with moving annular gratings resulted in prominent increase of induced gamma power under conditions of 'slow', 'medium' and 'fast' stimulus velocities in both child and adult samples (Fig. 2). In children, the strength of the gamma response increased between 6 and 15 years of age, while in adults it remained stable between 19 and 40 years of age (Tab.2, Fig. 7A). This developmental growth in the power of induced gamma oscillations was accompanied by a drop in their frequency that continues during adulthood but at a much slower pace (Tab.4 , Fig. 7B).

A developmental increase in the strength of visual gamma response is compatible with previous reports of a maturational rise in auditory gamma oscillations evidenced by increase in amplitude and/or inter-trial coherency of 40-Hz auditory steady-state responses (ASSR) (Cho, et al., 2015; Edgar, et al., 2016). Cho et al (Cho, et al., 2015) observed that the amplitude of the ASSRs increased in children between 8 and 16 years of age, but then dropped between 15-16 and 20-22 years. Although we had very few subjects within the 15 – 22 year age range, (which precludes statistical analysis of the latter effect), the presence of very high gamma response values in the older children in our sample and their absence in adults (Fig. 7A) suggests that the reduction of gamma amplitude between adolescence and early adulthood may be a common feature of both the auditory and visual cortices.

Several factors may underlie developmental changes in gamma response power. The main contributor might be the maturation of inhibitory GABAergic neurotransmission that in primates is protracted into early adulthood (Le Magueresse and Monyer, 2013). Changes in subunit composition of GABAR (GABA-Receptor) (Hashimoto, et al., 2009), as well as increasing 'on-demand' GABA release (Pinto, et al., 2010) produce a developmental shifts toward stronger, more precise inhibitory currents, thereby resulting in highly coherent activity of principal cells in the upper gamma frequency band (Doischer, et al., 2008).

Developmental slowing of the visual gamma oscillations observed in our study is in line with results of Gaetz and colleagues (Gaetz, et al., 2012) who reported a decrease in the frequency of gamma oscillations induced by static visual gratings in subjects aged 8-45 years. However, the small number of children (12 subjects) and much larger number of adults (47 subjects) included in their sample did not allow Gaetz et al. to perform a separate analysis of developmental trajectories in the maturing and the aging brain. Our study shows that the rate- and most probably the mechanism - of the developmental decrease in gamma frequency differ in children and adults.

The frequency of the induced gamma oscillations predominantly depends on the excitatory state of FS PV+ inhibitory neurons with higher frequency related to their higher tonic excitability (Anver, et al., 2011; Ferando and Mody, 2015; Mann and Mody, 2010). There is convincing evidence of a developmental shift towards lower NMDA-mediated tonic excitation of the FS PV+ cells, as well as of a developmental reduction of the number of FS PV+ cells exhibiting excitatory NMDA-mediated currents (Wang and Gao, 2009). On the other hand, tonic inhibitory regulation of the FS PV+ interneurons gradually increases during postnatal development (Le Magueresse and Monyer, 2013). These maturational transformations leading to subtler tonic excitability of inhibitory neurons may well explain

the highly pronounced and rapid decrease in the frequency of visual gamma oscillations that we observed between childhood and adolescence. Of note, the expression of the NMDAR units (NR1, NR2a, NR2b) proceeds to decrease even in the mature brain - from young to middle-aged adulthood (Adams, et al., 2008). These changes in NMDA transmission might explain the more gradual decrease of visual gamma frequency between 19 and 40 years of age in our study.

4.3. Modulation of gamma oscillations by excitatory drive.

Increasing velocity of visual motion from 1.2 to 6.0°/s (which also shifts the temporal frequency of the stimulation from 4 to 20 Hz) was associated with significantly stronger relative pupillary constriction (Fig. 1). It has been previously found that pupil constriction can be induced by changing attributes of a visual stimulation (e.g. spatial structure, color or motion coherence) without any changes in light flux (Barbur, et al., 1998; Sahraie and Barbur, 1997; Wilhelm, et al., 2002). These pupillary reactions are thought to reflect the activation of cortical areas involved in processing of respective features of the visual stimuli (Barbur, et al., 1998). In our paradigm, the increase in pupil constriction from slow to fast motion velocity is likely to reflect increasing activation of the motion-processing cortical areas (including V1, V5 and beyond) that in turn causes transient weakening of the central sympathetic inhibition of the parasympathetic Edinger-Westphal nucleus of the midbrain (Wilhelm, et al., 2002). Thus, the pupillometry findings support our interpretation of the effect of the motion velocity on gamma response as being a direct consequence of the rising excitatory drive to the visual cortex. The latter is further supported by the observation that the gratings moving at fast velocity were often perceived by the participants as most intense and even unpleasant.

Our results suggest that the frequency and power of induced gamma oscillations strongly depend on the strength of the excitatory drive. The increasing excitatory drive with increasing motion velocity from ‘slow’ to ‘fast’ lead to acceleration of gamma oscillations in all participants with reliably detectable gamma peaks (Fig. 4B). The mean increase in frequency was almost the same in children (15.3 Hz) and adults (14.6 Hz).

Experimental studies in animals (Mann and Mody, 2010), as well as simulation studies (Moca, et al., 2014), suggest that excitation of inhibitory FS interneurons is the main factor affecting the frequency of gamma oscillations. The recent DCM modeling study by Shaw and colleagues (Shaw, et al., 2017) has shown that reduction of gamma frequency by GABA reuptake inhibitor tiagabine is partly mediated by its effect on the time constant of

the inhibitory interneurons. Therefore, the increase in gamma frequency with speeding the visual motion might be at least partly mediated by increasing excitation of FS interneurons in response to increasing excitatory drive.

The gamma response power decreased with increasing motion velocity in all participants who had reliable gamma responses under the 'slow' condition, with the exception of three subjects (one adult and two children; Fig. 4A, dashed lines), all of whom had neurological conditions revealed post-hoc (epilepsy, Arnold-Chiari malformation, minor motor ticks and frequent nightmares). In the majority of the participants, regardless of their age, the gamma response decreased already in the transition from 'slow' to 'medium' velocity (see two examples in Fig. 5A), although in a few subjects the 'medium' velocity augmented the gamma response, which started to attenuate only under the 'fast' velocity condition (Fig. 5B).

The robustness of the gamma suppression with increasing velocity of visual motion as well as its overall similarity in children and adults suggest that this phenomenon is not age-specific and reflects a very basic mechanism underlying the generation of gamma oscillations in the visual cortex. Concurrently, as we mentioned in the introduction, the gamma suppression phenomenon is at odds with the results of other MEG studies that consistently reported increases in gamma response power with increasing excitatory drive to the visual cortex (Hadjipapas, et al., 2015; Hall, et al., 2005; Muthukumaraswamy and Singh, 2013; Peiker, et al., 2015; Perry, et al., 2015; Siegel, et al., 2007; Swettenham, et al., 2009).

The opposite behavior of gamma oscillations in our and other studies fits well the predictions from the Borgers and Kopell model (Borgers and Kopell, 2005) and may be explained by an inverted U-shaped relationship between strength of excitatory drive and power of gamma oscillations (Fig. 9). The reliable *enhancement* of gamma response observed in MEG studies that manipulated excitatory drive with luminance contrast (Hadjipapas, et al., 2015; Hall, et al., 2005; Perry, et al., 2015), eccentricity (van Pelt and Fries, 2013), motion coherence (Peiker, et al., 2015; Siegel, et al., 2007), or compared stationary and slowly moving stimuli (Muthukumaraswamy and Singh, 2013; Swettenham, et al., 2009) might be explained by a relatively weak excitation produced by such manipulations at the ascending portion of the bell-shaped curve (Fig. 9A).

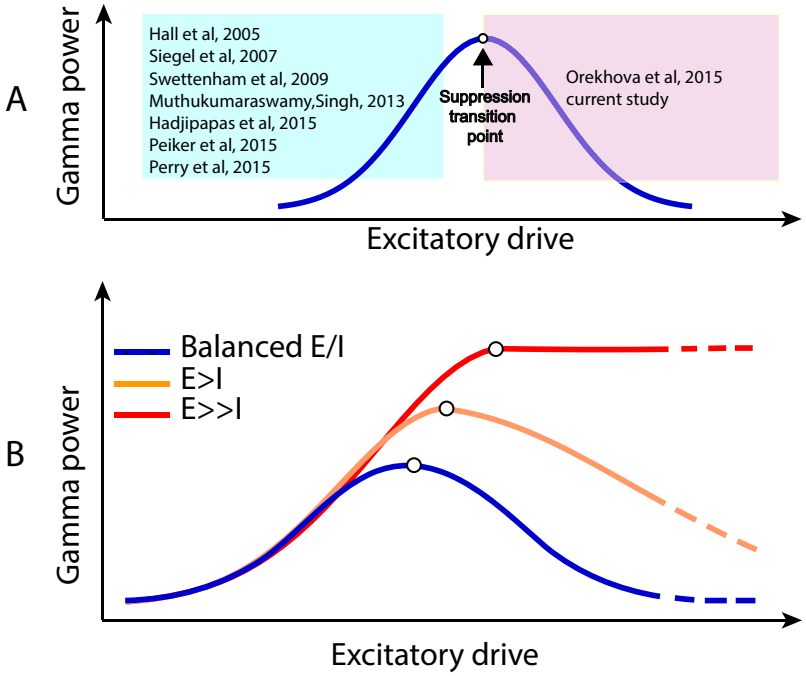

Figure 9. A hypothetical relationship between power of gamma response and strength of excitatory drive. **A**. Bell-shaped dependency of gamma power on the strength of excitatory drive. The previous reports on MEG gamma enhancement with increasing luminance contrast, motion coherence, decreasing eccentricity, or transition from stationary to slowly drifting gratings are compatible with the effects of modest stimulus intensity at the upward branch of the bell-shaped curve. In our studies suppression of the gamma response with increasing stimulus velocity has been induced by strong excitatory drive whose intensity was close to (slow velocity) or well above (fast velocity) the suppression transition point. **B**. The schematic representation of the effects of optimal (blue) and elevated (orange, red) E/I ratios on the gamma power modulation. The increased E/I ratio shifts the transition point towards higher excitatory drive and results in reduced or absent gamma power suppression.

At a certain high level of the external excitatory drive (the *'suppression transition point'*), when the FS cells are sufficiently excited, they lose their capacity to support gamma oscillations, since they either walk out of phase with pyramidal cells or desynchronize (Borgers and Kopell, 2005; Borgers and Walker, 2013; Cannon, et al., 2014). It is conceivable that in the majority of our subjects (with the exception of a few cases pictured in Fig. 5B and 5C), the excitatory drive produced by the 'slow' motion was close to or above the 'suppression transition point' and that the further increase of velocity up to the medium and high values put the visual networks in the high excitatory state corresponding to the descending portion of the bell-shaped curve, thus resulting in relative suppression of gamma response power.

Remarkably, the model by Borgers and Kopell explains while the PING gamma oscillations are not supported beyond the 30-90 Hz frequency range (Kopell, et al., 2010). Therefore, the gamma amplitude reduction in the 'fast' velocity condition is well in line with

acceleration of the visual gamma oscillations that approach the upper border of this range in response to the 'fast' velocity (especially in children, see Tab. 2).

4.4. Gamma suppression and its relation to the E/I balance in visual networks

The Borgers and Kopell's model states that the gamma suppression with increasingly strong excitatory drive occurs more easily when excitatory postsynaptic currents in pyramidal cells are well compensated by inhibitory ones (Borgers and Kopell, 2005). Therefore, one may expect that at the same level of a sufficiently high external excitatory drive, the gamma power suppression will be relatively stronger when there is stronger excitation of inhibitory neurons and/or weaker excitation of excitatory pyramidal cells (Fig. 9B). Since a greater tonic excitation of the inhibitory neurons also accelerates gamma oscillations (Mann and Mody, 2010), one can expect that individual variability in gamma suppression parameters and gamma frequency are partially controlled by the same neural mechanism. Therefore, individuals with higher gamma peak frequency should be likely to display greater velocity-related gamma power suppression, which also has a steeper slope, i.e. gamma power suppression peaks at a relatively lower excitatory drive. By the same token, both the magnitude and the slope of gamma suppression should be reduced in case of an elevated E/I ratio driven by either excessive excitation of excitatory circuitry or by relatively weak inhibition. The predicted link between gamma suppression parameters, gamma frequency and E/I balance was supported by our data in several ways.

First, we found the predicted positive correlations between gamma suppression parameters and peak gamma frequency (in children) or changes in frequency (in adults) (Table 4). The dissimilar pattern of the correlations may reflect low power of the analysis, but may also reflect different mechanisms of the E/I balance in the developing and mature brain.

Secondly, consistent with results of the previous behavioral (Melnick, et al., 2013) and proton magnetic resonance spectroscopy (H1-MRS) (Cook, et al., 2016) studies linking the strength of neural inhibition in the visual cortex with cognitive functions, we found that the stronger and faster gamma response suppression correlated with higher IQ in children (Tab. 6, Fig. 8). This correlation suggests that lower E/I ratio in the visual cortex in associated with better cognitive functioning in neurotypical children. It is however unclear if the E/I balance in the visual cortex is important by itself or as a reflection of the widespread E/I level in the brain. Absence of significant correlations between general IQ and gamma

suppression in adults suggests that an optimal E/I balance in the visual cortex might be less important for the general cognitive functioning of the mature brain.

Thirdly, the deviations from the typical gamma suppression values seemed to be associated with abnormally elevated E/I ratio in the visual cortex. Three out of 66 (39 children and 27 adults) participants with highly reliable gamma peaks in the 'slow' velocity condition failed to suppress gamma oscillations even at the highest velocity/excitatory drive (see Fig. 4C for the spectra of two of these subjects), and their post-hoc examination revealed neurological conditions that might be associated with cortical hyper-excitability (epilepsy, Arnold-Chiari malformation and a case with minor motor tics and frequent nightmares). Although more systematic investigation is warranted, these outliers' data are generally in line with the prediction that the low or absent gamma suppression at the descending branch of the bell-shaped curve is indicative of global imbalance in excitation within the visual cortical networks.

Of note, the unbalanced excitation in visual cortex of subjects with neuropsychiatric disorders might be reflected not only in an absent/reduced gamma power suppression at the descending branch of the bell-shaped curve, but also as an abnormal gamma power gain at its ascending branch. Indeed, Peiker et al (Peiker, et al., 2015) have found abnormally strong modulation of gamma power by gradually increasing coherence of visual motion in people with autism spectrum disorders. Investigation of gamma response modulation as a function of excitatory drive at both the ascending and descending branches of the bell-curve would add important knowledge about E/I balance in normal and atypical brain.

4.5. Gamma modulations and age

Highly reliable suppression of gamma power and increase of gamma frequency with increasing velocity of visual motion has been observed in both children and adults (Fig. 6). The developmental stability of the gamma modulations suggests that the global E/I balance under increasing excitatory drive is efficiently regulated in the healthy brain throughout the broad age range of subjects included in the study. Moreover, given the substantially higher gamma frequency in children as compared to adults (Tab. 1, Fig. 7B), the adjustment of the global E/I balance in the immature brain seems to be achieved at a higher level of excitability of both E and I neurons. The developmental stability of the gamma response modulations is in line with an *in vitro* observation that the number of inhibitory synapses on the neuronal branches scale together with the number of excitatory synapses during development, resulting in a relatively stable E/I ratio across several developmental stages (Liu, 2004).

However, a few words of caution are warranted regarding the lack of a reliable developmental trend in gamma modulation parameters. According to animal studies, the maturation of neural processes underlying the E/I balance in auditory and visual cortices takes place during early sensitive periods of brain development (Froemke, 2015). All of our participants were older than 6 years of age, and it is not unlikely that infants and toddlers would present gamma modulation parameters that are still age-dependent due to a continuing developmental fine-turning of the E/I balance in the visual cortex. This could also be true for the youngest children from our sample. These children were more frequently excluded from the gamma suppression analysis due to a low signal to noise ratio of the gamma response. While only including cases with highly reliable gamma responses in terms of signal-to-noise ratio allowed us to reduce the impact of noise on the gamma suppression parameters, it also lowered the proportion of youngest participants in our child sample.

5. Conclusions

Although a link between gamma oscillations and the E/I balance in neural networks is hardly disputable, the hope that the frequency or power of human gamma response may serve as a single non-invasive indicator of the E/I balance is perhaps overly simplistic. Here, we investigated the phenomenon of gamma power suppression caused by gradual increase in stimulus velocity in children and adults and provided evidence for its potential role as a putative biomarker of the E/I balance in the visual cortex. Our study resulted in two main novel findings.

First, we found a substantial developmental slowing of visual gamma oscillations from already 7 years of age, and that therefore cannot be explained by 'aging' (Gaetz, et al., 2012). This finding challenges the prevailing view, which predicts that maturational changes in neurotransmission should improve precision with which populational neural activity is synchronized and, as a result, increase both gamma synchronization and gamma frequency (Uhlhaas, et al., 2010). Given the animal data (Mann and Mody, 2010; Wang and Gao, 2009), the likely mechanism for developmental slowing of gamma oscillations is the developmental decrease in tonic excitability of the PV+ FS inhibitory neurons in the visual cortex. Functionally, given the role of inhibitory transmission in neural plasticity, faster juvenile visual gamma oscillations may be beneficial for perceptual learning, which proceeds with higher intensity in younger as compared to older brains.

The second novel finding is the developmental stability of the suppressive effect of an increasing velocity of visual motion on the strength of gamma response coupled with an

acceleration of gamma oscillations. Although the suppressive effect of excessively strong excitatory drive on MEG gamma power is well in line with the theoretical predictions (Borgers and Kopell, 2005; Cannon, et al., 2014), to our knowledge it has not been demonstrated before, with the exception of our earlier studies in children (Orekhova, et al., 2015; Stroganova, et al., 2015). Because gamma oscillations facilitate information transmission (Vinck, et al., 2013), their effective suppression with a 'too strong' excitatory drive may have a protective function via reducing the number of cortical assembles engaged in information flow and preventing cortical hyper-excitation in response to sensory stimuli.

Given that the slope of gamma suppression correlated with the frequency of the gamma response in the developing brain, we suggest that these parameters are sensitive to partly inter-related neural processes. However, while the frequency of gamma oscillations predominantly depends on the tonic excitability of inhibitory neurons (Mann and Mody, 2010), efficient gamma suppression may reflect a *global balance* between mutually counteracting excitatory and inhibitory circuits. The link between the magnitude of gamma suppression and IQ values in children points to the importance of an optimal E/I balance for cognitive abilities. A remarkable developmental stability of gamma suppression in healthy brain and its atypical absence in a small proportion of our participants with neurological abnormalities allow us to speculate that a gamma suppression deficit may characterize a disturbed E/I balance in the hyper-excitable visual cortex in individuals over a wide age range. Due to the lack of direct neurophysiological evidence in the context of the same 'visual motion' experimental paradigm, this interpretation should be treated with caution. However, it allows us to make several testable predictions for future research regarding functional consequences of individual variability in gamma suppression.

We expect that a gamma suppression deficit at the high levels of excitatory drive will characterize: patients with seizure onset zones located in the occipital cortex, neuro-typical individuals with visual hypersensitivity, and patients from clinical groups characterized by sensory modulation problems. Furthermore, a deficit in gamma suppression is likely to correlate with other non-invasive indexes of unbalanced excitation/inhibition in the visual cortex provided by, e.g., the H-MRS and visual perceptual tasks.

In conclusion, we suggest that velocity-related changes in gamma oscillations characterize individual variation in E/I balance and efficacy of neural inhibition in the visual cortex and may provide a valuable inhibition-based biomarker for patients with neuropsychiatric disorders.

Funding

This work is financed by Torsten Söderberg Foundation (M240/13to CG) and the Russian Scientific Foundation (14-35-00060 to TS). Authors JFS and BR are supported by the Knut and Alice Wallenberg Foundation (grant 2014.0102), the Swedish Research Council (grant 621-2012-3673), and the Swedish Childhood Cancer Foundation (grant MT2014-0007). The author NH was supported by the LifeWatch Foundation. The author TS was supported by the Charity Foundation "Way Out".

Acknowledgements

We heartily thank all participants and children families for their participation in this study.

We are grateful to Maria S. Davletshina and Anna V. Butorina for help with data collection.

References

Adams, M.M., Shi, L., Linville, M.C., Forbes, M.E., Long, A.B., Bennett, C., Newton, I.G., Carter, C.S., Sonntag, W.E., Riddle, D.R., Brunso-Bechtold, J.K. (2008) Caloric restriction and age affect synaptic proteins in hippocampal CA3 and spatial learning ability. Experimental Neurology, 211:141-149.

Anver, H., Ward, P.D., Magony, A., Vreugdenhil, M. (2011) NMDA Receptor Hypofunction Phase Couples Independent gamma-Oscillations in the Rat Visual Cortex. Neuropsychopharmacology, 36:519-528.

Barbur, J.L., Wolf, J., Lennie, P. (1998) Visual processing levels revealed by response latencies to changes in different visual attributes. Proceedings of the Royal Society B-Biological Sciences, 265:2321-2325.

Borgers, C., Kopell, N. (2005) Effects of noisy drive on rhythms in networks of excitatory and inhibitory neurons. Neural Computation, 17:557-608.

Borgers, C., Walker, B. (2013) Toggling between gamma-frequency activity and suppression of cell assemblies. Frontiers in Computational Neuroscience.

Buhl, E.H., Tamas, G., Fisahn, A. (1998) Cholinergic activation and tonic excitation induce persistent gamma oscillations in mouse somatosensory cortex in vitro. J Physiol, 513 (Pt 1):117-26.

Cannon, J., McCarthy, M.M., Lee, S., Lee, J., Borgers, C., Whittington, M.A., Kopell, N. (2014) Neurosystems: brain rhythms and cognitive processing. Eur J Neurosci, 39:705-719.

Carmignoto, G., Vicini, S. (1992) Activity-Dependent Decrease in Nmda Receptor Responses during Development of the Visual-Cortex. Science, 258:1007-1011.

Cho, R.Y., Walker, C.P., Polizzotto, N.R., Wozny, T.A., Fissell, C., Chen, C.M.A., Lewis, D.A. (2015) Development of Sensory Gamma Oscillations and Cross-Frequency Coupling from Childhood to Early Adulthood. Cereb Cortex, 25:1509-1518.

Cook, E., Hammett, S.T., Larsson, J. (2016) GABA predicts visual intelligence. Neurosci Lett, 632:50-4.

Doischer, D., Hosp, J.A., Yanagawa, Y., Obata, K., Jonas, P., Vida, I., Bartos, M. (2008) Postnatal Differentiation of Basket Cells from Slow to Fast Signaling Devices. Journal of Neuroscience, 28:12956-12968.

Dorrn, A.L., Yuan, K., Barker, A.J., Schreiner, C.E., Froemke, R.C. (2010) Developmental sensory experience balances cortical excitation and inhibition. Nature, 465:932-937.

Ecker, C., Spooren, W., Murphy, D.G.M. (2013) Translational approaches to the biology of Autism: false dawn or a new era? Mol Psychiatr, 18:435-442.

Edgar, J.C., Fisk, C.L., Liu, S., Pandey, J., Herrington, J.D., Schultz, R.T., Roberts, T.P.L. (2016) Translating Adult Electrophysiology Findings to Younger Patient Populations: Difficulty Measuring 40-Hz Auditory Steady-State Responses in Typically Developing Children and Children with Autism Spectrum Disorder. Developmental Neuroscience, 38:1-14.

Ferando, I., Mody, I. (2015) In vitro gamma oscillations following partial and complete ablation of delta subunit-containing GABA(A) receptors from parvalbumin interneurons. Neuropharmacology, 88:91-98.

Froemke, R.C. (2015) Plasticity of Cortical Excitatory-Inhibitory Balance. Annual Review of Neuroscience, Vol 38, 38:195-219.

Gaetz, W., Roberts, T.P.L., Singh, K.D., Muthukumaraswamy, S.D. (2012) Functional and structural correlates of the aging brain: Relating visual cortex (V1) gamma band responses to age-related structural change. Human Brain Mapping, 33:2035-2046.

Gramfort, A., Luessi, M., Larson, E., Engemann, D.A., Strohmeier, D., Brodbeck, C., Goj, R., Jas, M., Brooks, T., Parkkonen, L., Hamalainen, M. (2013) MEG and EEG data analysis with MNE-Python. Front Neurosci, 7:267.

Gross, J., Kujala, J., Hamalainen, M., Timmermann, L., Schnitzler, A., Salmelin, R. (2001) Dynamic imaging of coherent sources: Studying neural interactions in the human brain. P Natl Acad Sci USA, 98:694-699.

Hadjipapas, A., Lowet, E., Roberts, M.J., Peter, A., De Weerd, P. (2015) Parametric variation of gamma frequency and power with luminance contrast: A comparative study of human MEG and monkey LFP and spike responses. Neuroimage, 112:327-340.

Hall, S.D., Holliday, I.E., Hillebrand, A., Singh, K.D., Furlong, P.L., Hadjipapas, A., Barnes, G.R. (2005) The missing link: analogous human and primate cortical gamma oscillations. Neuroimage, 26:13-7.

Hashimoto, T., Nguyen, Q.L., Rotaru, D., Keenan, T., Arion, D., Beneyto, M., Gonzalez-Burgos, G., Lewis, D.A. (2009) Protracted Developmental Trajectories of GABA(A) Receptor alpha 1 and alpha 2 Subunit Expression in Primate Prefrontal Cortex. Biol Psychiatry, 65:1015-1023.

Hoogenboom, N., Schoffelen, J.M., Oostenveld, R., Parkes, L.M., Fries, P. (2006) Localizing human visual gamma-band activity in frequency, time and space. Neuroimage, 29:764-773.

Isaacson, J.S., Scanziani, M. (2011) How Inhibition Shapes Cortical Activity. Neuron, 72:231-243.

Jia, X.X., Xing, D.J., Kohn, A. (2013) No Consistent Relationship between Gamma Power and Peak Frequency in Macaque Primary Visual Cortex. Journal of Neuroscience, 33:17-U421.

Kaufman, A.S., Kaufman, N.L. (2004) KABC-II : Kaufman Assessment Battery for Children. 2nd ed. Circle Pines, MN: AGS Pub.

Kopell, N., Börgers, C., Pervouchine, D., Malerba, P., Tort, A. (2010) Gamma and Theta Rhythms in Biophysical Models of Hippocampal Circuits. In: Cutsuridis, V., Graham, B.P., Cobb, S., Vida, I., editors. Hippocampal Microcircuits: A Computational Modeller's Resource Book.: Springer p423-457.

Le Magueresse, C., Monyer, H. (2013) GABAergic Interneurons Shape the Functional Maturation of the Cortex. Neuron, 77:388-405.

LeBlanc, J.J., Fagiolini, M. (2011) Autism: A "Critical Period" Disorder? Neural Plasticity.

Lee, E., Lee, J., Kim, E. (2017) Excitation/Inhibition Imbalance in Animal Models of Autism Spectrum Disorders. Biol Psychiatry, 81:838-847.

Levin, A.R., Nelson, C.A. (2015) Inhibition-Based Biomarkers for Autism Spectrum Disorder. Neurotherapeutics, 12:546-52.

Liu, G. (2004) Local structural balance and functional interaction of excitatory and inhibitory synapses in hippocampal dendrites. Nature Neuroscience, 7:373-9.

Maheshwari, A., Noebels, J.L. (2014) Monogenic models of absence epilepsy: windows into the complex balance between inhibition and excitation in thalamocortical microcircuits. Genetics of Epilepsy, 213:223-252.

Mann, E.O., Mody, I. (2008) The multifaceted role of inhibition in epilepsy: seizure-genesis through excessive GABAergic inhibition in autosomal dominant nocturnal frontal lobe epilepsy. Current Opinion in Neurology, 21:155-160.

Mann, E.O., Mody, I. (2010) Control of hippocampal gamma oscillation frequency by tonic inhibition and excitation of interneurons. Nature Neuroscience, 13:205-U90.

Melnick, M.D., Harrison, B.R., Park, S., Bennetto, L., Tadin, D. (2013) A strong interactive link between sensory discriminations and intelligence. Curr Biol, 23:1013-7.

Moca, V.V., Nikolic, D., Singer, W., Muresan, R.C. (2014) Membrane resonance enables stable and robust gamma oscillations. Cereb Cortex, 24:119-42.

Munk, M.H., Roelfsema, P.R., Konig, P., Engel, A.K., Singer, W. (1996) Role of reticular activation in the modulation of intracortical synchronization. Science, 272:271-4.

Muthukumaraswamy, S.D., Singh, K.D. (2013) Visual gamma oscillations: The effects of stimulus type, visual field coverage and stimulus motion on MEG and EEG recordings. Neuroimage, 69:223-230.

Muthukumaraswamy, S.D., Singh, K.D., Swettenham, J.B., Jones, D.K. (2010) Visual gamma oscillations and evoked responses: Variability, repeatability and structural MRI correlates. Neuroimage, 49:3349-3357.

Nelson, S.B., Valakh, V. (2015) Excitatory/Inhibitory Balance and Circuit Homeostasis in Autism Spectrum Disorders. Neuron, 87:684-698.

Orekhova, E.V., Butorina, A.V., Sysoeva, O.V., Prokofyev, A.O., Nikolaeva, A.Y., Stroganova, T.A. (2015) Frequency of gamma oscillations in humans is modulated by velocity of visual motion. J Neurophysiol, 114:244-255.

Peiker, I., Schneider, T.R., Milne, E., Schottle, D., Vogeley, K., Munchau, A., Schunke, O., Siegel, M., Engel, A.K., David, N. (2015) Stronger Neural Modulation by Visual Motion Intensity in Autism Spectrum Disorders. PLoS One, 10:e0132531.

Perry, G. (2015) The effects of cross-orientation masking on the visual gamma response in humans. Eur J Neurosci, 41:1484-1495.

Perry, G., Randle, J.M., Koelewijn, L., Routley, B.C., Singh, K.D. (2015) Linear Tuning of Gamma Amplitude and Frequency to Luminance Contrast: Evidence from a Continuous Mapping Paradigm. PLoS One, 10.

Piekarski, D.J., Johnson, C.M., Boivin, J.R., Thomas, A.W., Lin, W.C., Delevich, K., E, M.G., Wilbrecht, L. (2017) Does puberty mark a transition in sensitive periods for plasticity in the associative neocortex? Brain Res, 1654:123-144.

Pinto, J.G.A., Hornby, K.R., Jones, D.G., Murphy, K.M. (2010) Developmental changes in GABAergic mechanisms in human visual cortex across the lifespan. Frontiers in Cellular Neuroscience.

Roberts, M.J., Lowet, E., Brunet, N.M., Ter Wal, M., Tiesinga, P., Fries, P., De Weerd, P. (2013) Robust Gamma Coherence between Macaque V1 and V2 by Dynamic Frequency Matching. Neuron, 78:523-536.

Rossiter, H.E., Worthen, S.F., Witton, C., Hall, S.D., Furlong, P.L. (2013) Gamma oscillatory amplitude encodes stimulus intensity in primary somatosensory cortex. Front Hum Neurosci, 7.

Rubenstein, J.L.R., Merzenich, M.M. (2003) Model of autism: increased ratio of excitation/inhibition in key neural systems. Genes Brain and Behavior, 2:255-267.

Sahraie, A., Barbur, J.L. (1997) Pupil response triggered by the onset of coherent motion. Graefes Arch Clin Exp Ophthalmol, 235:494-500.

Schadow, J., Lenz, D., Thaerig, S., Busch, N.A., Frund, I., Herrmann, C.S. (2007a) Stimulus intensity affects early sensory processing: Sound intensity modulates auditory evoked gamma-band activity in human EEG. International Journal of Psychophysiology, 65:152-161.

Schadow, J., Lenz, D., Thaerig, S., Busch, N.A., Frund, I., Rieger, J.W., Herrmann, C.S. (2007b) Stimulus intensity affects early sensory processing: Visual contrast modulates evoked gamma-band activity in human EEG. International Journal of Psychophysiology, 66:28-36.

Shaw, A.D., Moran, R.J., Muthukumaraswamy, S.D., Brealy, J., Linden, D.E., Friston, K.J., Singh, K.D. (2017) Neurophysiologically-informed markers of individual variability and pharmacological manipulation of human cortical gamma. Neuroimage, 161:19-31.

Siegel, M., Donner, T.H., Oostenveld, R., Fries, P., Engel, A.K. (2007) High-frequency activity in human visual cortex is modulated by visual motion strength. Cereb Cortex, 17:732-741.

Stroganova, T.A., Butorina, A.V., Sysoeva, O.V., Prokofyev, A.O., Nikolaeva, A.Y., Tsetlin, M.M., Orekhova, E.V. (2015) Altered modulation of gamma oscillation frequency by speed of visual motion in children with autism spectrum disorders. J Neurodev Disord. p 21.

Swettenham, J.B., Muthukumaraswamy, S.D., Singh, K.D. (2009) Spectral Properties of Induced and Evoked Gamma Oscillations in Human Early Visual Cortex to Moving and Stationary Stimuli. J Neurophysiol, 102:1241-1253.

Takada, N., Pi, H.J., Sousa, V.H., Waters, J., Fishell, G., Kepecs, A., Osten, P. (2014) A developmental cell-type switch in cortical interneurons leads to a selective defect in cortical oscillations. Nature Communications.

Tan, H.R.M., Gross, J., Uhlhaas, P.J. (2016) MEG sensor and source measures of visually induced gamma-band oscillations are highly reliable. Neuroimage, 137:34-44.

Taulu, S., Hari, R. (2009) Removal of magnetoencephalographic artifacts with temporal signal-space separation: demonstration with single-trial auditory-evoked responses. Hum Brain Mapp, 30:1524-34.

Tzourio-Mazoyer, N., Landeau, B., Papathanassiou, D., Crivello, F., Etard, O., Delcroix, N., Mazoyer, B., Joliot, M. (2002) Automated anatomical labeling of activations in SPM using a macroscopic anatomical parcellation of the MNI MRI single-subject brain. Neuroimage, 15:273-289.

Uhlhaas, P.J., Roux, F., Rodriguez, E., Rotarska-Jagiela, A., Singer, W. (2010) Neural synchrony and the development of cortical networks. Trends Cogn Sci, 14:72-80.

van Pelt, S., Boomsma, D.I., Fries, P. (2012) Magnetoencephalography in Twins Reveals a Strong Genetic Determination of the Peak Frequency of Visually Induced Gamma-Band Synchronization. Journal of Neuroscience, 32:3388-3392.

van Pelt, S., Fries, P. (2013) Visual stimulus eccentricity affects human gamma peak frequency. Neuroimage, 78:439-447.

Vinck, M., Womelsdorf, T., Fries, P. (2013) Gamma-band synchronization and information transmission. In: Quiroga, R.Q., Panzeri, S., editors. Principles of Neural Coding: CRC Press. p 449-469.

Wang, H.X., Gao, W.J. (2009) Cell Type-Specific Development of NMDA Receptors in the Interneurons of Rat Prefrontal Cortex. Neuropsychopharmacology, 34:2028-2040.

Wechsler, D. (2010) WAIS IV: Wechsler Adult Intelligence Scale – Fourth Edition. Svensk version. NCS Pearson Inc. .

Wilhelm, B.J., Wilhelm, H., Moro, S., Barbur, J.L. (2002) Pupil response components: studies in patients with Parinaud's syndrome. Brain, 125:2296-2307.

Wu, Y., Liu, D., Song, Z. (2015) Neuronal Networks and Energy Bursts in Epilepsy. Neuroscience, 287:175-186.

Xue, M.S., Atallah, B.V., Scanziani, M. (2014) Equalizing excitation-inhibition ratios across visual cortical neurons. Nature, 511:596-600.

Yizhar, O., Fenno, L.E., Prigge, M., Schneider, F., Davidson, T.J., O'Shea, D.J., Sohal, V.S., Goshen, I., Finkelstein, J., Paz, J.T., Stehfest, K., Fudim, R., Ramakrishnan, C., Huguenard, J.R., Hegemann, P., Deisseroth, K. (2011) Neocortical excitation/inhibition balance in information processing and social dysfunction. Nature, 477:171-178.